

terms proportional to $r_a - c$ and $r_b - c$, separately. Equation (13), whose right-hand side can be written $(1 - \eta_a)(1 - \eta_b) - (\eta_a - \zeta_a)(\eta_b - \zeta_b)$, is proportional to $(r_a - c)(r_b - c)$, but with an inaccurate proportionality constant. For $r_a = r_b$, Eq. (6) becomes

$$Z = \eta(1 + \zeta)^{-1}. \quad (14)$$

The term $(1 + \zeta)^{-1}$ is the analog of Bethe's $(1 + 2\zeta)^{-1}$ which he attributes to an excluded volume effect. Since there ought to be no such effect in the present problem, the factor must instead be a mathematical artifact.

At middle distances, ζ will be small while η is still appreciable. There, neither approximation reproduces the term $\eta_a \eta_b$ in the exact solution, since both give $1 - \eta_a - \eta_b$ for Ψ .

Table I gives the values of the wave function at $r_a = r_b$ for the three solutions. The off-diagonal values show a similar behavior, and it is not instructive to

TABLE I. Values of the wave function.

$r_a = r_b$ (F)	Exact	Bethe [Eq. (7)]	Day [Eq. (13)]
0.4	0	0	0
0.45	0.0265	0.0228	0.0112
0.5	0.0844	0.0634	0.0464
0.6	0.2262	0.1784	0.1647
0.8	0.4772	0.4302	0.4273
1.0	0.6485	0.6214	0.6209

reproduce them here. The wave function was computed for $\gamma_\eta = 1.2 \text{ F}^{-1}$, $\gamma_\zeta = 4.4 \text{ F}^{-1}$, and $c = 0.4 \text{ F}$. It will be seen that the Bethe approximation is generally much closer than the Day to the exact solution. The conclusion of both authors that the three-body effects in nuclear matter are small, is not, of course, affected by the inaccuracies of their approximations, but the effect of a short-range attraction would be underestimated, more severely by Day than by Bethe.

Deuteron Elastic Scattering from He^3 and H^3 †

T. A. TOMBRELLO, R. J. SPIGER, AND A. D. BACHER
California Institute of Technology, Pasadena, California

(Received 10 October 1966)

The elastic scattering of deuterons from He^3 and H^3 has been studied for bombarding energies up to 11 MeV. The excitation curves obtained show a broad resonance in the scattering cross section corresponding to an excitation energy of 20 ± 0.5 MeV in both He^5 and Li^5 . These data, together with $\text{H}^3(d, n)\text{He}^4$ and $\text{He}^3(d, p)\text{He}^4$ data from other sources, tend to indicate that D waves are responsible for the anomaly.

INTRODUCTION

AT present the well-established levels of Li^5 or He^5 are the $\frac{3}{2}^-$ ground state, the $\frac{1}{2}^-$ first excited state, and the $\frac{3}{2}^+$ level that lies just above the deuteron threshold. No structure that could correspond to other excited states has been seen in either $^1\text{He}^4(n, n)\text{He}^4$ or $^2,3\text{He}^4(p, p)\text{He}^4$ above the position of the $\frac{3}{2}^+$ levels.⁴ However, a broad anomaly at an excitation energy of ~ 20 MeV has been observed in the yield curves for $\text{H}^3(d, n)\text{He}^4$.^{5,6} Studies of the $\text{He}^3(d, p)\text{He}^4$ reaction at

widely spaced energies confirm these results,⁷ and the proton polarization from this reaction is quite large in this energy region.⁸

Previous experimental results for the $\text{H}^3 + d$ and $\text{He}^3 + d$ elastic-scattering reactions either have been limited to low bombarding energies^{9,10} or have been available only at widely spaced points.¹¹ With this in mind, the present data were obtained with the hope that a clearer insight into the origin of the broad anomaly might be gained. The data presented here overlap with the previous low-energy work, and extend to a deuteron bombarding energy of 11 MeV, which corresponds to a maximum excitation energy of about 23 MeV in the compound nuclei. The excitation curves

† Supported in part by the Office of Naval Research [Nonr-220(47)].

¹ R. E. Shamu and J. G. Jenkin, Phys. Rev. **135**, B99 (1964); R. E. Benenson, D. B. Lightbody, A. Sayres, and W. E. Stephens, Bull. Am. Phys. Soc. **10**, 52 (1965).

² P. W. Allison and R. Smythe, Bull. Am. Phys. Soc. **9**, 544 (1964); P. W. Allison, Ph.D. thesis, University of Colorado, 1965 (unpublished).

³ H. E. Conzett, Bull. Am. Phys. Soc. **11**, 25 (1966).

⁴ T. Lauritsen and F. Ajzenberg-Selove, Nucl. Phys. **78**, 1 (1966).

⁵ S. J. Bame and J. E. Perry, Phys. Rev. **107**, 1616 (1957).

⁶ M. D. Goldberg and J. M. LeBlanc, Phys. Rev. **122**, 164 (1961).

⁷ L. Stewart, J. E. Brolley, and L. Rosen, Phys. Rev. **119**, 1649 (1960).

⁸ R. I. Brown and W. Haerberli, Phys. Rev. **130**, 1163 (1963).

⁹ R. J. S. Brown, K. F. Famularo, H. D. Holmgren, D. Rankin, and T. F. Stratton, Phys. Rev. **96**, 80 (1954).

¹⁰ W. F. Stratton, G. D. Freier, G. R. Keepin, D. Rankin, and T. F. Stratton, Phys. Rev. **88**, 257 (1952).

¹¹ J. E. Brolley, T. M. Putnam, L. Rosen, and L. Stewart, Phys. Rev. **117**, 1307 (1960).

for both elastic-scattering reactions are quite similar and clearly show the broad resonance-like structure at an excitation energy of about 20 MeV. Using these data, together with the $H^3(d,n)He^4$ and $He^3(d,p)He^4$ data from other sources,⁵⁻⁷ one obtains an indication that D waves are responsible for the anomaly.

APPARATUS AND DATA, He^3+d

Data were obtained using both the $He^3(d,d)He^3$ and $d(He^3,He^3)d$ reactions, though the major portion of the final results comes from the former. The scattering chamber employed has been described in detail previously,¹² so only a brief description will be given here.

The scattering volume is 28 cm in diameter and is isolated from the vacuum system by a 1000 Å nickel foil before the beam collimator and by a 5000 Å foil in front of the Faraday cup. The target pressure was maintained at $\sim 1/60$ atm and was measured with an oil-filled manometer and a cathetometer.

The detector collimator had an angular resolution of $\pm 1.8^\circ$, and the accuracy of the angular position was better than $\pm 0.1^\circ$. The detection system consisted of a 50- μ surface-barrier detector and a 3-mm lithium-drifted silicon detector. This telescope was used to separate the singly- and doubly-charged reaction products except at the lowest energies, where only the kinematic separation of the deuterons and He^3 's could be used to resolve them.

Deuteron bombarding energies between 2 and 11 MeV were employed, and He^3 bombarding energies between 4 and 12.5 MeV. The uncertainty in the energies given is about ± 25 keV. The overall precision of the values of the differential cross section is about $\pm 5\%$ including the statistical uncertainty, which was always less than

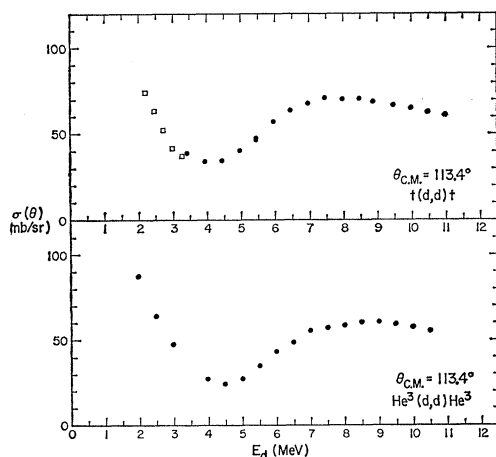


FIG. 1. The differential cross sections for $H^3(d,d)H^3$ and $He^3(d,d)He^3$ at a center-of-mass scattering angle of 113.4° . The solid circles are data from the present work; the open squares are interpolated values from Ref. 10.

¹² T. A. Tombrello and L. S. Senhouse, Phys. Rev. **129**, 2252 (1963).

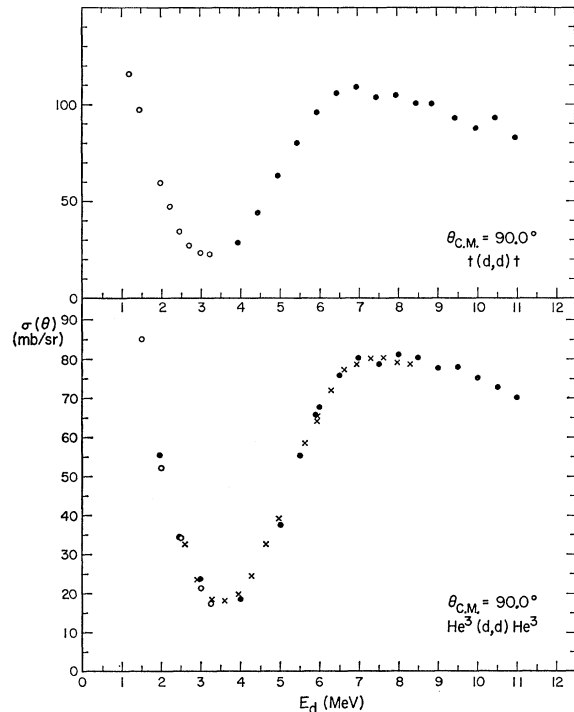


FIG. 2. The differential cross sections for $H^3(d,d)H^3$ and $He^3(d,d)He^3$ at a center-of-mass angle of 90.0° . The solid circles are our data for $H^3(d,d)H^3$ and $He^3(d,d)He^3$; the open circles are data from Refs. 9 and 10; and the crosses are our data for $d(He^3,He^3)d$.

1.5%. The cross sections are tabulated in Tables I and II, and selected excitation curves are given in Figs. 1-5. Where these results overlap those of Brown *et al.*⁹ the agreement is seen to be excellent.

TABLE I. The center-of-mass cross sections for the elastic scattering of He^3 from deuterium. The bombarding energy has been converted to an equivalent deuteron bombarding energy to facilitate the comparison of these data with those in Table II.

E_d (MeV)	$\sigma(37.8^\circ)$ (mb/sr)	$\sigma(71.0^\circ)$ (mb/sr)	$\sigma(90^\circ)$ (mb/sr)	$\sigma(125.2^\circ)$ (mb/sr)	$\sigma(150^\circ)$ (mb/sr)
2.59	211.4	...	32.6	104.6	248.6
2.93	173.7	33.7	23.6	91.9	265.3
3.27	149.7	31.2	18.5	82.8	279.1
3.61	142.2	29.3	18.0	74.3	296.5
3.95	138.0	31.8	19.7	67.0	303.0
4.28	143.0	34.2	24.5	61.5	309.7
4.62	159.5	36.0	32.8	54.8	320.4
4.95	178.5	38.6	39.1	51.2	317.9
5.63	226.0	41.2	58.5	43.7	296.5
5.93	248.3	43.4	64.0	43.1	282.3
5.96	251.4	43.5	65.4	42.4	284.3
6.30	272.9	43.8	72.1	40.7	262.4
6.63	287.1	43.1	77.3	39.6	249.6
6.96	302.1	41.6	78.7	37.6	219.8
7.30	318.2	40.5	80.3	37.1	209.6
7.63	319.6	38.4	80.6	35.1	200.1
7.97	315.3	37.1	79.2	34.6	195.3
8.30	280.2	35.0	78.9	33.2	202.8

TABLE II. The center-of-mass cross sections for the elastic scattering of deuterons from He^3 .
The deuteron energy is in the laboratory system.

E_d (MeV)	$\sigma(33.2^\circ)$ (mb/sr)	$\sigma(44.4^\circ)$ (mb/sr)	$\sigma(54.8^\circ)$ (mb/sr)	$\sigma(73.1^\circ)$ (mb/sr)	$\sigma(90^\circ)$ (mb/sr)	$\sigma(113.4^\circ)$ (mb/sr)	$\sigma(125.2^\circ)$ (mb/sr)	$\sigma(140^\circ)$ (mb/sr)
1.96	442.1	150.0	84.9	54.9	55.5	87.6	123.5	184.5
2.48	262.3	108.8	65.3	39.2	34.2	64.0	108.0	190.6
2.98	56.4	32.1	23.7	47.3
3.48	154.3	80.8	...	27.4	84.6	196.1
3.98	141.0	85.7	53.6	28.2	18.5	27.6	70.7	190.7
4.48	143.6	89.7	56.6	24.7	61.5	185.4
4.99	171.9	104.1	58.5	39.1	37.6	27.4	54.9	175.3
5.49	205.8	114.1	59.3	42.6	55.4	35.0	48.1	159.2
5.89	44.5	65.8
5.99	249.4	133.4	59.2	45.8	67.7	43.3	46.2	144.4
6.49	295.3	141.1	56.9	42.5	75.9	48.6	41.8	124.1
6.99	334.2	157.3	56.6	43.8	80.3	55.6	39.9	106.0
7.49	353.9	162.1	56.9	41.5	78.8	57.2	37.9	89.2
7.99	360.3	162.9	58.9	39.7	81.2	58.2	35.1	71.7
8.49	370.6	162.6	55.3	37.0	80.4	60.7	32.7	...
8.99	376.5	164.6	54.8	36.1	77.8	60.8	31.5	...
9.49	382.3	163.6	52.8	32.9	78.1	59.3	29.2	...
9.99	379.6	162.1	51.0	30.4	75.3	57.5
10.49	378.9	161.8	49.3	30.5	72.7	55.3
10.99	379.6	162.8	49.0	28.8	70.1

APPARATUS AND DATA, H^3+d

A complete description of the scattering chamber is available,¹³ and we will content ourselves with only a general outline of its characteristics. In size and configuration it is quite similar to that used for $\text{He}^3(d,d)\text{He}^3$; however, instead of the entrance and exit foils used in that experiment, the tritium gas was contained in a small

central gas cell (5 cm in diameter). This cell had an entrance window of 8200-Å thick nickel and 13 000-Å nickel exit windows. A target pressure of $\sim 1/20$ atm was used and was measured with a Wallace-Tiernan differential pressure gauge.

The detector collimator had an angular resolution of $\pm 1^\circ$, and angles could be set with an accuracy of about $\pm 0.05^\circ$. Reaction products were detected and identified with a counter telescope composed of 26- μ and 2-mm thick surface-barrier detectors.

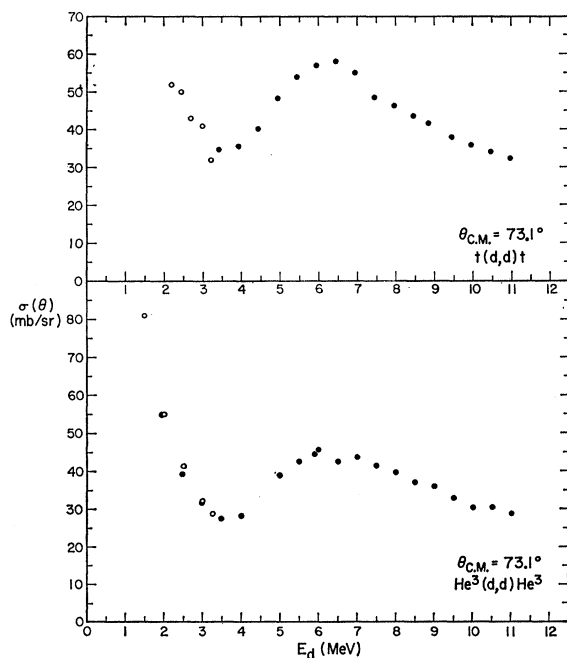


FIG. 3. The differential cross sections for $\text{H}^3(d,d)\text{H}^3$ and $\text{He}^3(d,d)\text{He}^3$ at a center-of-mass angle of 73.1° . The symbols have the same significance as those in Fig. 2.

¹³ R. J. Spiger, Ph.D. thesis, California Institute of Technology, 1967 (unpublished).

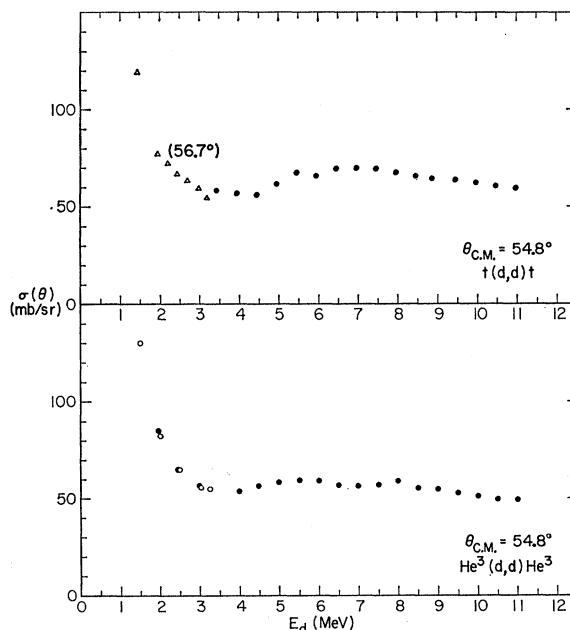


FIG. 4. The differential cross sections for $\text{H}^3(d,d)\text{H}^3$ and $\text{He}^3(d,d)\text{He}^3$ at a center-of-mass angle of 54.8° . The solid circles are our data; the open circles are from Ref. 9; the open triangles are $\text{H}^3(d,d)\text{H}^3$ data from Ref. 10 at a center-of-mass angle of 56.7° .

TABLE III. The center-of-mass cross sections for the elastic scattering of deuterons from tritium. The deuteron energy is in the laboratory system.

E_d (MeV)	$\sigma(54.8^\circ)$ (mb/sr)	$\sigma(73.1^\circ)$ (mb/sr)	$\sigma(90.0^\circ)$ (mb/sr)	$\sigma(113.4^\circ)$ (mb/sr)
3.43	58.2	34.8	...	38.8
3.94	56.9	35.6	28.5	34.0
4.44	56.4	40.2	43.9	34.6
4.94	61.9	48.2	63.0	40.6
5.45	66.0	54.0	79.8	46.2
	67.3			47.6
5.95	69.5	57.0	95.6	57.4
6.45	69.8	58.1	105.4	64.1
6.96	69.4	55.0	108.8	68.0
7.46	69.4	48.5	103.5	71.2
7.96	67.7	46.4	104.1	70.3
8.46	65.6	43.5	100.3	70.5
8.86	64.2	41.7	99.9	68.9
9.46	63.5	37.9	92.3	66.8
9.96	62.0	35.9	87.1	65.2
10.47	60.5	34.1	92.7	62.9
10.97	59.1	32.5	82.6	61.2

Because tritium gas exchanges readily with normal hydrogen in hydrogenous materials, contamination is always a serious problem. Though an effort was made to minimize contact with such materials, some hydrogen contamination took place. The fraction of normal hydrogen within the target gas was determined by comparing the yield of recoil protons with that obtained when the target cell was filled entirely with normal hydrogen. This fraction was constant at a value of ~ 0.1 during the course of the $\text{H}^3(d,d)\text{H}^3$ measurements.

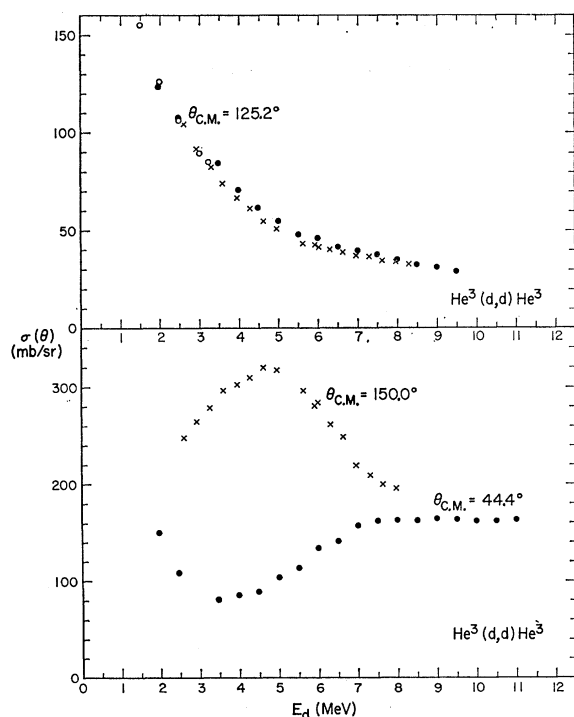


FIG. 5. The differential cross sections for $\text{He}^3(d,d)\text{He}^3$ and $d(\text{He}^3,\text{He}^3)d$ for center-of-mass angles 44.4° , 125.2° , and 150.0° . The solid circles are our $\text{He}^3(d,d)\text{He}^3$ data; the crosses are our $d(\text{He}^3,\text{He}^3)d$ data; the open circles are data from Ref. 9.

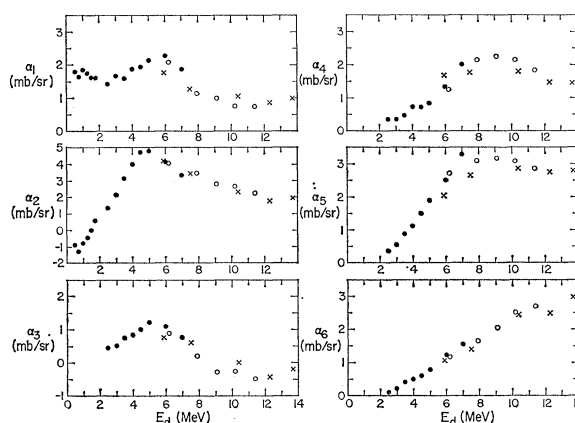


FIG. 6. The coefficients of the Legendre polynomial expansion of the center-of-mass angular distributions for $\text{H}^3(d,n)\text{He}^4$ [solid circles (Ref. 5); open circles (Ref. 6)] and for $\text{He}^3(d,p)\text{He}^4$ [crosses (Ref. 7)]. a_l is the coefficient of $P_l(\cos\theta_{e.m.})$ in the expansion.

Deuteron bombarding energies between 3.5 and 11 MeV were used, and energies given have an uncertainty of ± 25 keV. The precision of the differential-cross-section values is estimated to be about $\pm 6\%$, including the statistical uncertainty, which was always less than 1.5%. These values of the cross sections are given in Table III and are displayed in Figs. 1–4. Where these results can be compared with those of Stratton *et al.*,¹⁰ they are in good agreement.

DISCUSSION

As seen in Figs. 1–4, the excitation curves for the two elastic-scattering reactions are quite similar. Most of the curves clearly show the broad resonance observed previously by Bame and Perry in the $\text{H}^3(d,n)\text{He}^4$ reaction.⁵ Several important features should be noted: the pronounced interference effect seen at $\theta_{e.m.} = 90.0^\circ$ (Fig. 2), which rules out a negative-parity assignment for the resonance, and the rather featureless behavior observed at 54.8° (Fig. 4) and at 125.2° (Fig. 5). Because the particles involved have nonzero spins, no theoretical importance can be attached to the near-disappearance of the resonance at these zeros of $P_2(\cos\theta_{e.m.})$; however, the smoothness of these curves as contrasted with those at other angles tends to raise the suspicion that D waves are involved.

Usually one relies on a phase-shift analysis of the data to untangle the resonant and nonresonant partial waves. In this case, however, it seems out of the question to perform such an analysis for the following reasons:

(1) The spins of the two particles involved require a large number of independent elements of the scattering matrix, and thereby require many independent experiments (polarization, spin-correlation, etc.) to uniquely specify the results of the analysis.

(2) The complexity of the problem is increased by the presence of an open two-body reaction channel and

two open three-body channels that all have appreciable cross sections.

We must, therefore, extract what information we can without recourse to this most general method.

Further insight may be obtained by considering the behavior of the coefficients of the Legendre polynomial expansion of the angular distributions for H³(*d,n*)He⁴ and He³(*d,p*)He⁴. These results are taken entirely from the original sources⁵⁻⁷ and are displayed in Fig. 6. (Only the coefficients for *P*₁ through *P*₆ are shown.) Notice that a resonance is seen in α₁, α₂, and α₃ for a deuteron energy of 5-6 MeV; α₄ and α₅ also show a broad peak but at a somewhat higher energy, 8-9 MeV. The large anomaly in α₂ demonstrates that the resonance has *l* > 0, and together with our elimination of the odd values of *l* using the behavior of the elastic scattering, the only reasonable choice remaining is *l* = 2.

As an aid to understanding the behavior of these coefficients, we consider the angular distribution *W*(θ) for this reaction which would be produced by an isolated *D*-wave resonance (no background). (Refer to the Appendix for the most general formula.)

$$\begin{aligned} J^\pi = \frac{7}{2}^+, \quad S = \frac{3}{2}: \quad W(\theta) &= 4/49(27P_4 + 50P_2 + 49), \\ J^\pi = \frac{5}{2}^+, \quad S = \frac{3}{2}: \quad W(\theta) &= 3/49(-48P_4 + 20P_2 + 49), \\ J^\pi = \frac{3}{2}^+, \quad S = \frac{3}{2}: \quad W(\theta) &= 2, \\ J^\pi = \frac{1}{2}^+, \quad S = \frac{3}{2}: \quad W(\theta) &= 1, \\ J^\pi = \frac{5}{2}^+, \quad S = \frac{1}{2}: \quad W(\theta) &= 3/7(6P_4 + 8P_2 + 7), \\ J^\pi = \frac{3}{2}^+, \quad S = \frac{1}{2}: \quad W(\theta) &= 2(P_2 + 1), \end{aligned}$$

where *J* is the total angular momentum of the resonance, π is its parity, and *S* is the channel spin.

The occurrence of weak anomalies in the coefficients of *P*₁ and *P*₃ probably corresponds to interference with odd-parity partial waves in the nonresonant background. The strong effect seen in α₂ excludes an assignment of $\frac{1}{2}^+$ (⁴*D*_{1/2}); in the same way, an assignment of $\frac{3}{2}^+$ with pure *S* = $\frac{3}{2}$ (⁴*D*_{3/2}) would also be unlikely. Since α₄ does not resonate in the energy range corresponding to the anomaly, one would also tend to rule out $\frac{7}{2}^+$

(⁴*D*_{7/2}). Thus, if there is only one resonance in this energy range, the only remaining assignments are $\frac{3}{2}^+$ or $\frac{5}{2}^+$, where in the latter case a particular channel spin mixture would be necessary to cancel the coefficient of *P*₄. Either choice would have an appreciable *S* = $\frac{1}{2}$ component and would thus be at least partly of the form ²*D*_{3/2} or ²*D*_{5/2}.¹⁴ This result is surprising, since if this state is thought of as being formed by coupling the 3⁺ first excited state of Li⁶ to a 1*s* hole, then one would expect a $\frac{7}{2}^+$ or $\frac{5}{2}^+$ state that was mainly ⁴*D*.

In making these arguments based on the behavior of Legendre coefficients, one has no real assurance that more than one *D*-wave level is not involved or that a broad *S*-wave level could not be "buried" in the background. Thus, the conclusions concerning the spin of this anomaly cannot be taken seriously unless we can be sure that only one level is present.

Recently, more information about this region of excitation has become available from the Li⁷(*p*,He³)He⁵ and Li⁷(*p*,*t*)Li⁵ data of Cerny *et al.*¹⁵ Making use of the selection rule on the allowed relative spin orientation of the nucleons picked up in these reactions, the formation of a state with *S* = $\frac{3}{2}$ is permitted only for the (*p*,He³) reaction. The validity of this selection rule is confirmed by the observation of the $\frac{3}{2}^+$ state at 16.70 MeV in He⁵ but not the mirror state in Li⁵. Similarly, they observe a broad 20-MeV state in He⁵ and not in Li⁵ and thus conclude that this level must have *S* = $\frac{3}{2}$. This result would lead to an assignment of ⁴*D* for a single level, but since *S* = $\frac{3}{2}$ would not be consistent with the behavior of the Legendre coefficients, it would appear that there may be several *D*-wave excited states in He⁵ and Li⁵ in this energy region.

ACKNOWLEDGMENTS

The authors would like to express their appreciation to the following for their help with the data reduction: F. Bacher, A. Tombrello, D. Papanastassiou, and R. Moore. We also wish to acknowledge conversations with J. Cerny and R. McGrath concerning their experimental results.

APPENDIX

The following formulas give the differential cross section for a reaction involving particles with spins of 1 and $\frac{1}{2}$ in the initial state, and with spins of 0 and $\frac{1}{2}$ in the final state. Also given is an expression for the spin polarization of the resulting spin- $\frac{1}{2}$ particle.

$$\sigma(\theta) = \frac{1}{3}(|a|^2 + |b|^2 + |c|^2 + |d|^2 + |e|^2 + |f|^2),$$

where

$$\begin{aligned} a = \frac{\sin\theta}{2k} \sum_l P_l'(\cos\theta) \left\{ \left[\frac{l-1}{2(2l-1)} \right]^{1/2} S_{(\beta, l, \frac{1}{2}; \alpha, l-2, \frac{1}{2})}^{l-\frac{1}{2}} + (l+2) \left[\frac{3}{2l(2l+3)} \right]^{1/2} S_{(\beta, l, \frac{1}{2}; \alpha, l, \frac{1}{2})}^{l+\frac{1}{2}} \right. \\ \left. + (l-1) \left[\frac{3}{2(l+1)(2l-1)} \right]^{1/2} S_{(\beta, l, \frac{1}{2}; \alpha, l, \frac{1}{2})}^{l-\frac{1}{2}} + \left[\frac{l+2}{2(2l+3)} \right]^{1/2} S_{(\beta, l, \frac{1}{2}; \alpha, l+2, \frac{1}{2})}^{l+\frac{1}{2}} \right\}, \end{aligned}$$

¹⁴ T. A. Tombrello, A. D. Bacher, and R. J. Spiger, Bull. Am. Phys. Soc. **10**, 423 (1965).

¹⁵ J. Cerny, C. Détraz, and R. H. Pehl, Phys. Rev. **152**, 950 (1966).

$$b = \frac{\sin^2 \theta}{2k} \sum_l P_l''(\cos \theta) \left\{ \left[\frac{1}{2(2l-1)(2l-1)} \right]^{1/2} S_{(\beta, l, \frac{1}{2}; \alpha, l-2, \frac{1}{2})}^{l-\frac{1}{2}} - \left[\frac{3}{2l(2l+3)} \right]^{1/2} S_{(\beta, l, \frac{1}{2}; \alpha, l, \frac{1}{2})}^{l+\frac{1}{2}} \right. \\ \left. + \left[\frac{3}{2(l+1)(2l-1)} \right]^{1/2} S_{(\beta, l, \frac{1}{2}; \alpha, l, \frac{1}{2})}^{l-\frac{1}{2}} - \left[\frac{1}{2(l+2)(2l+3)} \right]^{1/2} S_{(\beta, l, \frac{1}{2}; \alpha, l+2, \frac{1}{2})}^{l+\frac{1}{2}} \right\},$$

$$c = \frac{\sin \theta}{2k} \sum_l P_l'(\cos \theta) \left\{ \left[\frac{l-1}{2(2l-1)} \right]^{1/2} S_{(\beta, l, \frac{1}{2}; \alpha, l-2, \frac{1}{2})}^{l-\frac{1}{2}} - \left[\frac{l}{6(2l+3)} \right]^{1/2} S_{(\beta, l, \frac{1}{2}; \alpha, l, \frac{1}{2})}^{l+\frac{1}{2}} - \left[\frac{l+1}{6(2l-1)} \right]^{1/2} S_{(\beta, l, \frac{1}{2}; \alpha, l, \frac{1}{2})}^{l-\frac{1}{2}} \right. \\ \left. + \left[\frac{l+2}{2(2l+3)} \right]^{1/2} S_{(\beta, l, \frac{1}{2}; \alpha, l+2, \frac{1}{2})}^{l+\frac{1}{2}} + \sqrt{\frac{2}{3}} S_{(\beta, l, \frac{1}{2}; \alpha, l, \frac{1}{2})}^{l+\frac{1}{2}} - \sqrt{\frac{2}{3}} S_{(\beta, l, \frac{1}{2}; \alpha, l, \frac{1}{2})}^{l-\frac{1}{2}} \right\},$$

$$d = \frac{1}{2k} \sum_l P_l(\cos \theta) \left\{ -l \left[\frac{l-1}{2(2l-1)} \right]^{1/2} S_{(\beta, l, \frac{1}{2}; \alpha, l-2, \frac{1}{2})}^{l-\frac{1}{2}} - (l+1) \left[\frac{l}{6(2l+3)} \right]^{1/2} S_{(\beta, l, \frac{1}{2}; \alpha, l, \frac{1}{2})}^{l+\frac{1}{2}} \right. \\ \left. + l \left[\frac{l+1}{6(2l-1)} \right]^{1/2} S_{(\beta, l, \frac{1}{2}; \alpha, l, \frac{1}{2})}^{l-\frac{1}{2}} + (l+1) \left[\frac{l+2}{2(2l+3)} \right]^{1/2} S_{(\beta, l, \frac{1}{2}; \alpha, l+2, \frac{1}{2})}^{l+\frac{1}{2}} \right. \\ \left. + (l+1) \sqrt{\frac{2}{3}} S_{(\beta, l, \frac{1}{2}; \alpha, l, \frac{1}{2})}^{l+\frac{1}{2}} + l \sqrt{\frac{2}{3}} S_{(\beta, l, \frac{1}{2}; \alpha, l, \frac{1}{2})}^{l-\frac{1}{2}} \right\},$$

$$e = \frac{1}{2k} \sum_l P_l(\cos \theta) \left\{ -l \left[\frac{l-1}{2l-1} \right]^{1/2} S_{(\beta, l, \frac{1}{2}; \alpha, l-2, \frac{1}{2})}^{l-\frac{1}{2}} - (l+1) \left[\frac{l}{3(2l+3)} \right]^{1/2} S_{(\beta, l, \frac{1}{2}; \alpha, l, \frac{1}{2})}^{l+\frac{1}{2}} + l \left[\frac{l+1}{3(2l-1)} \right]^{1/2} S_{(\beta, l, \frac{1}{2}; \alpha, l, \frac{1}{2})}^{l-\frac{1}{2}} \right. \\ \left. + (l+1) \left(\frac{l+2}{2l+3} \right)^{1/2} S_{(\beta, l, \frac{1}{2}; \alpha, l+2, \frac{1}{2})}^{l+\frac{1}{2}} - (l+1) \sqrt{\frac{1}{3}} S_{(\beta, l, \frac{1}{2}; \alpha, l, \frac{1}{2})}^{l+\frac{1}{2}} - l \sqrt{\frac{1}{3}} S_{(\beta, l, \frac{1}{2}; \alpha, l, \frac{1}{2})}^{l-\frac{1}{2}} \right\},$$

and

$$f = \frac{\sin \theta}{2k} \sum_l P_l'(\cos \theta) \left\{ \left(\frac{l-1}{2l-1} \right)^{1/2} S_{(\beta, l, \frac{1}{2}; \alpha, l-2, \frac{1}{2})}^{l-\frac{1}{2}} - \left[\frac{l}{3(2l+3)} \right]^{1/2} S_{(\beta, l, \frac{1}{2}; \alpha, l, \frac{1}{2})}^{l+\frac{1}{2}} - \left[\frac{l+1}{3(2l-1)} \right]^{1/2} S_{(\beta, l, \frac{1}{2}; \alpha, l, \frac{1}{2})}^{l-\frac{1}{2}} \right. \\ \left. + \left[\frac{l+2}{(2l+3)} \right]^{1/2} S_{(\beta, l, \frac{1}{2}; \alpha, l+2, \frac{1}{2})}^{l+\frac{1}{2}} - \sqrt{\frac{1}{3}} S_{(\beta, l, \frac{1}{2}; \alpha, l, \frac{1}{2})}^{l+\frac{1}{2}} + \sqrt{\frac{1}{3}} S_{(\beta, l, \frac{1}{2}; \alpha, l, \frac{1}{2})}^{l-\frac{1}{2}} \right\}.$$

$$P(\theta) = \frac{2 \operatorname{Im}(ab^* + c^*d + ef^*)}{|a|^2 + |b|^2 + |c|^2 + |d|^2 + |e|^2 + |f|^2} \text{ in the direction of } (\hat{k}_{\text{in}} \times \hat{k}_{\text{out}}).$$

In the above formulas, k is the wave number for the relative motion in the initial state; \hat{k}_{in} and \hat{k}_{out} are unit vectors in the directions of motion of the incident and outgoing particles, respectively. The $S^J_{(\beta, l', s'; \alpha, l, s)}$ are elements of the scattering matrix that connect the initial channel α having orbital angular momentum l and channel spin s with the final channel β (different than α) having orbital angular momentum l' and channel spin s' . These expressions were obtained from the general form given by Bloch,¹⁶ but the signs of all the $S^J_{(\beta, l, \frac{1}{2}; \alpha, l+2, \frac{1}{2})}$ and $S^J_{(\beta, l, \frac{1}{2}; \alpha, l-2, \frac{1}{2})}$ have been changed to give the proper time-reversal invariance of the scattering matrix.

¹⁶ C. Bloch, *La théorie des réactions nucléaires* (Commissariat à l'Énergie Atomique, Service de Documentation, Saclay, France, 1955).